Acta Neuropathologica Communications

RESEARCH

Open Access

Curative timed NK cell-based immunochemotherapy aborts brain tumour recurrence driven by mesenchymal glioma stem cells

Brian Meehan[1], Lata Adnani[1], Xianbing Zhu[2], Nadim Tawil[1], Delphine Garnier[3], Ichiro Nakano[4], Sidong Huang[2] and Janusz Rak[1*]

Abstract

High grade gliomas (HGG) are incurable brain cancers, where inevitable disease recurrence is driven by tumour-initiating glioma stem cells (GSCs). GSCs survive and expand in the brain after surgery, radiation and temozolomide (TMZ) chemotherapy, amidst weak immune and natural killer (NK) cell surveillance. The present study was designed to understand how to enhance the contribution of innate immunity to post TMZ disease control. Strikingly, molecular subtypes of HGG impacted the repertoire of NK cell sensitivity markers across human HGG transcriptomes, and in a panel of GSCs with either proneural (PN-GSC) or mesenchymal (MES-GSC) phenotypes. Indeed, only MES-GSCs (but not PN-GSCs) were enriched for NK cell ligands and sensitive to NK-mediated cytotoxicity in vitro. While NK cells alone had no effect on HGG progression in vivo, the post-chemotherapy (TMZ) recurrence of MES-GSC-driven xenografts was aborted by timed intracranial injection of live or irradiated NK (NK92MI) cells, resulting in long term survival of animals. This curative effect declined when NK cell administration was delayed relative to TMZ exposure pointing to limits of the immune control over resurging residual tumour stem cell populations that survived chemotherapy. Overall, these results suggest that chemotherapy-dependent tumour depopulation may create a unique window of opportunity for NK-mediated intervention with curative effects restricted to a subset of HGGs driven by mesenchymal brain tumour initiating cells.

Keywords High grade glioma, Glioblastoma, Mesenchymal glioma stem cells, Proneural glioma stem cells, NK cells, Temozolomide, Molecular subtypes of glioma, Relapse, Intracranial immunotherapy, Intracranial xenografts

*Correspondence:
Janusz Rak
janusz.rak@mcgill.ca
[1]Research Institute of the McGill University Health Centre, 1001 Decarie Boul, Montreal, QC H4A 3J1, Canada
[2]Goodman Cancer Institute, McGill University, Montreal, QC, Canada
[3]Sorbonne University, Paris, France
[4]Department of Neurosurgery, Hokuto Social Medical Corporation, Hokuto Hospital, Kisen-7-5 Inadacho, Obihiro 080-0833, Hokkaido, Japan

Introduction

High grade glioma (HGG), including grade III and grade IV (glioblastoma) tumours comprise a class of incurable and highly invasive primary brain malignancies, associated with rapid progression and poor median overall survival [51]. These dismal outcomes have not radically improved during the past several decades in spite of implementation of aggressive treatment protocols involving surgical resection, radiation and chemotherapy, mostly with temozolomide (TMZ) [51]. While this intensive standard of care offers a transient disease-free respite, it is invariably followed by recurrence of molecularly altered, drug resistant and ultimately lethal malignancy [48], a natural history that can be modelled using patient-derived glioma stem cell xenografts in immune deficient mice [20].

The extensive ongoing research efforts aiming to better understand HGG pathogenesis and to overcome the related therapeutic challenges revealed a remarkable molecular heterogeneity and the existence of multiple subtypes of these disease states [38, 51]. For example, in adult glioblastoma (GBM) current classification distinguishes proneural (PN), classical (CL) and mesenchymal (MES) tumour subtypes based on the analysis of cellular transcriptomes, in parallel with the distinct repertoires of oncogenic mutations [51]. These global properties are superimposed with a complex cellular architecture within individual lesions, as documented by single cell gene expression profiling technologies [34] and functional studies suggesting the existence of cells with diverse tumour initiating potentials [30].

Molecular investigations have also reinforced the notion that the post-therapy relapse profoundly changes tumour characteristics [20, 48] and that throughout this process HGG masses contain rich infiltrates of reactive glial, inflammatory and vascular cells closely intertwined with the biology of the evolving disease [34, 49]. While these findings point to several possible therapeutic targets in primary or recurrent HGG, including oncogenic signalling pathways [51], blood vessels growth mechanisms [8] or immune checkpoints [14], their inspired clinical explorations did not lead to decisive improvements in patients' overall survival, for reasons that still remain incompletely understood.

In this regard, one of the striking features of the HGG-associated cellular microenvironment is the scarcity of immune effector cells, including CD4 + and CD8 + T cells, plasma cells, B cells, resting and activated natural killer (NK) cells and other cellular populations [49]. This property is attributed to several factors, such as systemic impairment of the immune cell recruitment into the central nervous system (CNS) sanctuary [13], blood-brain barrier (BBB) function of the vascular wall [39], immune cell exhaustion [44], or the immunologically 'cold' nature of the HGG-associated multicellular milieu [18]. Hence, considerable efforts are currently underway to overcome some of these impediments and improve the efficacy of immunotherapy in HGG patients [27]. The related strategies include eliciting a more immunostimulatory tumour microenvironment [18], anti-tumour vaccines [26], oncolytic viriotherapy [9], improving the penetration of immune cells across the BBB [39, 45], delivery of engineered chimeric antigen receptor T cells (CAR T) [3, 11, 12], intracranial immunotherapy [6, 17], or targeting intracellular mechanisms of tumour cell-related immune evasion [19].

While these efforts have largely focused on antigen-specific anticancer immunity [27], there is also a growing interest in exploiting the unique features of NK cells in the context of HGG therapy [22]. In contrast to cytotoxic T cells that are directed at 'non-self' traits of target cancer cells and subjected to multilayered negative regulation, NK cells are programmed to recognize and kill 'stressed' cells. Their canonical cellular targets often express low levels of major histocompatibility class I (MHC I) antigens, and include multiple types of cancer cells [31]. With their ostensibly greater ability to penetrate into the tumour tissue [22] NK cells can also trigger cytokine production, recruit other immune cells and induce tumour cell death or dormancy [15]. They engage their targets through an array of activating NK cell receptors (NKG2D, NKG2C, DNAM1), which recognize the corresponding ligands on the surface of cancer cells (MICA, MICB, ULBP1–6; HLA-E; or CD122, PVR/CD155, respectively). This interaction initiates the killing process that involves specialized proteins, such as perforin, granzyme A and granzyme B [23, 31].

It is notable in this context that only a restricted subset of HGG cells is now thought to possess full tumour initiating potential, including the ability to trigger disease recurrence [43]. These cells, often referred to as glioma stem cells (GSCs), exhibit a level of molecular and phenotypic diversity that gave rise to their assignment to either proneural (PN-GSC) or mesenchymal (MES-GSC) subsets [4, 30], which transcriptionally resemble the aforementioned GBM subtypes [30]. In this regard, PN-GSCs are reminiscent of the molecular repertoire of neural stem cells and form relatively slow growing, radiation sensitive tumours in immune deficient mice [2, 4, 20, 30]. In contrast, MES-GSCs form highly aggressive intracranial lesions, which tend to be radiation resistant, but are often relatively sensitive to TMZ chemotherapy [20, 30]. Whether GSC subtypes and their tumour-initiating potentials are equally affected by endogenous, or therapeutic NK cells along the HGG natural history remains largely unexplored.

Here we show that unlike their PN-GSC counterparts, the isolated MES-GSCs express a considerable repertoire

of ligands for activating NK receptors, and consequently, they exhibit a heightened susceptibility to NK-mediated killing in vitro. While the status of NK cells in mice inoculated with GSCs does not influence tumour take and progression, the disease relapse post TMZ therapy is aborted in NK cell-proficient (but not NK-deficient) mice. Similarly, intracranial injections of engineered human NK (NK92MI) cells timed following TMZ-induced cytoreduction blocks the relapse of orthotopic MES-GSC xenografts. These results suggest that NK cells may be exploited for curative purposes during the specific windows of time during HGG therapy and in a manner dependent on the tumour driving GSC subtype.

Materials and methods

Cell culture

Patient-derived mesenchymal human GSCs: GSC1123, GSC83 and proneural human GSCs: GSC157, GSC528 and GSC84 were generated from surgical HGG isolates in the laboratory of Dr. I. Nakano and were previously characterized for the status of isocitrate dehydrogenase (IDH1/2) gene mutation [30], O^6 methylguanine methyltransferase (MGMT) and other parameters [20]. The cells were maintained as deep frozen stocks and cultured for minimal required number of passages (less than 20) before use in experiments. Single cell RNA sequencing (scRNAseq) performed for another project has also validated their maintained gene expression and cellular complexity. K562 cell line was a kind gift from Dr. Kolja Eppert (McGill U.). NK92MI cells were purchased from the American Type Culture Collection (ATCC, CRL2408).

Animals

NSG [NSG IL2rg-/-] mice (NOD.Cg-Prkdc^{SCID}IL-2rg^{tm1Wjl}SzJ (Strain: 005557)) were purchased from Jackson Laboratories. Homozygous SCID mice harboring the YFP transgene or Fox Chase SCID mice CB17/Icr-*Prkdc*^{scid}/IcrIcoCrl (Strain:236) were bred at the RIMUHC [47]. Balanced numbers of male and female mice were used in our experiments based on availability. All mouse experiments were performed in accordance with the Canadian Council of Animal Care guidelines, and Animal Use Protocol (AUP#5200) approved by the Animal Care Committee of the Research Institute of McGill University Health Center.

Transcriptome analysis

The microarray data were downloaded from: https://www.ncbi.nlm.nih.gov/geo/query/acc.cgi?acc=GSE67089. The Cancer Genome Atlas (TCGA) bulk glioblastoma (GBM) transcriptome dataset was analyzed for repertoire of NK ligands using R2 Genomics Analysis and Visualization Platform (http://www.r2.amc.nl) for proneural (PN), classical (CL) and mesenchymal (MES) GBM subtypes. Data were analyzed as described in Supplementary Methods.

Flow cytometry

Flow cytometry was performed as detailed in Supplementary Methods, using indicated antibodies. Readings of the FACS Canto (BD) instrument were plotted as Mean Fluorescence Intensity (MFI) using with FloJo software (version 10.7.1).

Treatments in vitro

Responses of cultured cells to chemotherapy or radiation were analyzed using trypan blue exclusion assay, MTS assay and cell cycle profiling, as indicated in corresponding sections of Supplementary Methods.

NK cytotoxicity assay

The NK activity assay was based on the published protocol [25] involving a bioluminescent (BLI) read out. Briefly, Luciferase transduced GSCs were diluted to 3×10^5 cells per mL with GSC media and 100 µL of the cell suspension were placed in triplicate wells of a 96-well white flat-bottomed plate (Costar, 3912). NK92MI cells, or NK92MI-IR cells were added at indicated ratios and bioluminescence was measured using GloMax luminometer, as detailed in Supplementary Methods.

Mouse NK cell isolation and cell killing assay

The protocol was adapted from Wong et al. (2021) [53]. Basically, Fox Chase SCID mice were injected 18 h prior to the collection of spleens with 150 µg of Poly I: C (ALX-746-021-M002, Cedarlane Labs) in 200 µL of DPBS for activation of NK cells. Mice were then anesthetized, sacrificed after which the spleens were removed and placed in cold complete NK media, which consisted of RPMI164 (350-007-CL, Wisent), 10% FBS, Penicillin-Streptomycin, mouse IL-15 (447-ML-010, RnD Systems) and B-mercaptoethanol (M3148, Sigma) kept on ice. Three spleens per batch were placed on a 70 µm mesh (22363548, Fisher Scientific) inside of a petri dish with 3 mL of ACK lysis buffer (A10492-01, GIBCO) and mechanically dispersed using a 3 mL syringe piston. The dispersed cell mixture was collected by adding 12 mL of FACS buffer; containing 0.5% BSA, 2mM EDTA, in DPBS, with a sterile pipette and placed in a 15 mL tube. The tube was centrifuged at 300xg for 5 min and the supernatant was decanted. Another 2 mL of ACK lysis buffer was added to the pellet and the pellet was dispersed using a pipette or brief vortexing followed by filtration through a 40 µm mesh filter to remove large debris. The tube was centrifuged once again at 300xg for 5 min and the pellet was resuspended in 500 uL of FACS buffer. The cells were counted using an automatic cell counter Nexcelom (Aut

T4, Nexcelom Biosciences). Cells were aliquoted centrifuged at 300xg for 10 min resuspended in 40 uL of FACS buffer for every 10^8 cells. Next, 10 uL of MACS mouse NK cell biotin- antibody cocktail from the NK cell isolation kit (130-115-818, Miltenyi Biotech) was added to the cell suspension and was mixed by gentle pipetting then placed in the refrigerator for 5 min on a rocking shaker. After 5 min the cells were resuspended in 1.4 mL of FACS buffer then centrifuged at 300xg for 10 min. The pellets were resuspended in 80 uL of FACS solution for 10^8 cells and mixed with 20 uL of Antibody Biotin Cocktail coated beads for every 10^8 cells prior to incubation for 10 min at 4° C on a rocking shaker. The staining was terminated by addition of 600 uL of FACS solution to increase the volume prior to separation. NK cell isolation was carried out using an LS magnetic column (130-042-401, Miltenyi Biotec), which was prepared by placing it in the magnet and rinsing with 3 mL of FACS buffer. The collection tube was discarded and replaced with a fresh tube then the cell sample was added to the magnetic column. Once the sample volume had entered the column the column was washed with 3 rounds of 3 mL volumes of FACS buffer to collect the flow-through of the unbound mouse NK cells. The collection tube was then centrifuged at 300xg for 10 min and the supernatant decanted. The NK cells were resuspended in 500 uL of FACS buffer and the cells were counted using Trypan blue to establish viability. The NK cells were diluted to establish a 40:1 effector/target ratio and then serial dilutions were prepared at 20:1, 10:1, 5:1 and 2.5:1 effector to target cell ratios with indicated GSCs as targets. GSCs were kept constant at 3×10^3 cells per well. NK cells were loaded into the V-shaped bottom 96 well plate (249935, Corning) at distance from each other using one plate per dilution. Target cells (GSC1123bfpLuc) were collected and counted to achieve 3×10^4 cells per mL of complete RPMI media. Then 3×10^3 of these cells were added per well to the wells containing the mouse NK cells. The plates were then centrifuged at 100xg for one minute and placed in the incubator at 37° C for 2 h. At the end of the first 2 h incubation, 25 uL of Luciferin at 75µg/mL (122799, Perkin-Elmer) was added to each well containing cells and the luminescence was measured using the Glomax 96 microplate luminometer (Promega). The plates were placed back in the incubator for another 2 h. At the conclusion of the 4 hour period the bioluminescence in plates was measured once again until the maximum readings were determined. The plates were then returned to the incubator for overnight incubation and measurement the next morning following addition of fresh Luciferin as described above.

FACS analysis of mouse NK cells

Splenocytes, as well as purified mouse NK cells were placed in vials containing 100 µL of FACS media. Cells were stained on ice for 30 min with anti-mouse CD335-APC (NKp46) antibody (137608, Biolegend), anti-mouse CD3-FITC antibody (100204, Biolegend) and rat anti-mouse IgG2a-APC (400512, Biolegend). The cells were centrifuged for 5 min at 200xg and then washed once with 1 mL of Dulbecco Phosphate Buffered Saline (DPBS). The samples were transferred to FACS tubes (352054, Falcon) and analyzed on the FACS CANTO (BD Biosciences) as described.

NK92MI dilution assay in vivo

In order to determine whether at different effector/target ratios NK cells could curtail tumour initiating capacity of mesenchymal GSCs, both cell populations were mixed and inoculated intracranially, into immune deficient mice and tumour progression was monitored by bioluminescence (BLI) and symptom free survival. Thus, 2.5×10^4 of freshly harvested GSC1123bfpLuc (target) cells were either injected alone ($n = 10$), or upon admixture with NK92MI-IR cells at 10-fold excess (2.5×10^5 cells; $n = 9$) or at 80-fold excess (2×10^6 cells: $n = 5$). The mice were placed back in the cage and monitored through BLI (Revvity Spectrum 2) at regular intervals for a minimum of 30 days. The radiance (*p/sec/cm²/str)* was plotted, and a Kaplan-Meier survival curve was calculated. Statistics were calculated using the Gehan-Breslow-Wilcoxon method for curve comparison.

Xenografts

Treatment effects were analysed in both intracranial (i.c.) and subcutaneous (s.c.) xenograft models. To generate subcutaneous tumours, SCID or NSG mice were briefly anesthetized with isoflourane/oxygen and 2×10^6 cancer cells were injected subcutaneously into the left flank of each mouse as described [20]. To systemically deplete endogenous mouse NK cells, Anti-AsialoGM1 rabbit polyclonal antibody (100 uL/injection; Biolegend, 146002) was injected once per week intravenously into SCID mice beginning two weeks prior to tumour implantation and continued for another nine weeks. For intracranial implantation, anaesthetized SCID mice were injected with 2.5×10^4 of indicated GSCs and/or 2×10^6 NK92MI or NK92MI-IR cells (or indicated doses of NK92MI-EVs and at indicated times post chemotherapy) using Stoelting Stereotactic apparatus (Stoelting, 51733D). Intracranial tumours were monitored using IVIS Spectrum (Perkin Elmer) bioluminescent scanner [20]. Intraperitoneal TMZ therapy (120 mg/kg or 200 mg/kg or corresponding diluent: 1% DMSO in DPBS) commenced once the lesions reached a threshold bioluminescence as described in Supplementary Methods.

Tissue immunostaining

Tumour tissues were preserved using 4% paraformaldehyde in PBS, embedded in paraffin blocks, sectioned, stained with indicated antibodies and signal quantified (see Supplementary Methods).

Statistical analysis

Statistical analysis was performed using Prism 5.1 (GraphPad) package. Biological replicates were performed (3 or more), and sources of error (SD, SEM) were reported on the graph while *p* values were reported in figures, legends, or in a separate table. Statistical tests used included, as indicated, unpaired t tests, one-way analyses of variance (ANOVA) with post hoc analysis, multiple comparisons tests. Kaplan Meier Curve Comparison testing was performed by Prism using the Gehan-Breslow-Wilcoxon Test.

Results

Differential expression of NK receptor ligands by proneural and mesenchymal human glioma stem cells

Given the aggressive and recurrent nature of HGG we sought to understand whether the susceptibility of tumour-driving GSCs to NK-mediated killing may explain the apparent failure of innate immune surveillance in this disease. For this purpose, we interrogated the available gene expression databases of PN- or MES-GSCs isolated from brain tumours comprising multiple HGG subtypes [30], along with control normal human astrocytes [30], for known activating, multifunctional, or inhibitory ligands able to engage critical NK cell receptors [23, 41]. Notably, global transcriptomes revealed a clear separation of these cell lines into distinct clusters around either astrocytes, PN-GSCs, or MES-GSCs, thus highlighting their molecular heterogeneity (Fig. 1A). While there was some variability in the expression of mRNA for specific NK activating ligands between individual GSC lines, the levels of these transcripts were almost uniformly higher for MES-GSCs than for their PN-GSC counterparts, regardless of the nature of the original HGG isolate. This difference included MICA, MICB, ULBP1 and ULBP2, which are the canonical activators of the NKG2D receptor on NK cells (Fig. 1B) [23]. A similar, albeit less obvious, trend was observed in the case of multifunctional and inhibitory NK ligands (Fig. 1C and fig. S1). It is noteworthy that the molecular classification of hitherto characterized GSCs into PN and MES populations is predicated on their transcriptomic similarity to corresponding subtypes of grade IV HGG with wild type status of the IDH1/2 genes, currently classified as glioblastoma (GBM) [30, 51]. It should also be noted that GBM also includes a classical (CL) molecular subtype, in addition to PN and MES tumours [51] but GSCs in our series did not contain a corresponding transcriptome [20, 30]. To assess whether these bulk GBM transcriptomes would also differ with respect to NK ligands (as do GSCs) we performed in silico analysis of their corresponding mRNA profiles using the Cancer Genome Atlas (TCGA) database (fig. S2A). Indeed, MES GBM samples expressed considerably more of some (MICA and MICB), but not all transcripts encoding NK ligands relative to their PN counterparts, and there were also differences in MICA between CL and PN GBM tissues (fig. S2-S3). These observations suggest that MES transcriptome is enriched in NK ligands, both in bulk GBM and in isolated GSCs.

We have also examined PN- or MES-GSCs for NK ligand protein levels and functionality (Fig. 1D-F). We carried out some of these experiments in the presence or absence of temozolomide to account for the realities of GBM therapy (fig. S4). In this regard, flow cytometry analysis of NKG2D ligands, such as MICA and ULBP2/5/6 (Fig. 1D, E; fig. S5A-C and fig. S6), and DNAM1 ligand, PVR/CD155 (fig. S5C, S7), demonstrated their preferential and abundant expression by MES-GSCs [29], but not by PN-GSCs. MICB was not detectable on the surface of either GSC subtype (fig. S5B) [10]. While TMZ exposure was suggested to increase the responsiveness of GBM cells to NK-mediated cytotoxicity [10, 50] we observed no major changes in levels of key NK cell ligands (Fig. 1D, E; fig. S5A, B) in the presence of physiological and biologically effective concentrations [21, 35] of the drug (fig. S4). Also under in vivo growth conditions, in GSC xenografts, the levels of MICA remained markedly elevated in MES-GSC tumours relative to PN-GSC lesions, and did not observably change following the exposure of tumour bearing mice to TMZ, as determined by quantitative flow cytometry (Fig. 2; fig. S8).

Finally, we used the bioluminescence cytotoxicity assays [25] to explore more directly the effect of the engineered human NK cell line (NK92MI) against a panel of the aforementioned GSCs in culture. Remarkably, while all MES-GSC lines were efficiently killed by NK92MI cells across a wide range of effector-to-target ratios, their PN-GSC counterparts remained completely unaffected by human NK effectors (Fig. 1F, fig. S9, tab. S1). Overall, these results suggest that the intrinsic molecular subtype of GSCs represents a notable determinant of their cellular sensitivity to NK-mediated cytotoxicity, with MES-GSCs being especially susceptible to such killing.

Elevated sensitivity of mesenchymal glioma stem cells to NK-mediated surveillance post chemotherapy in vivo

In order to determine whether differential sensitivity to NK cell-mediated killing in vitro translates into corresponding antitumour responses in vivo, PN-GSCs and MES-GSCs were used to generate subcutaneous xenografts in strains of mice, which were either proficient

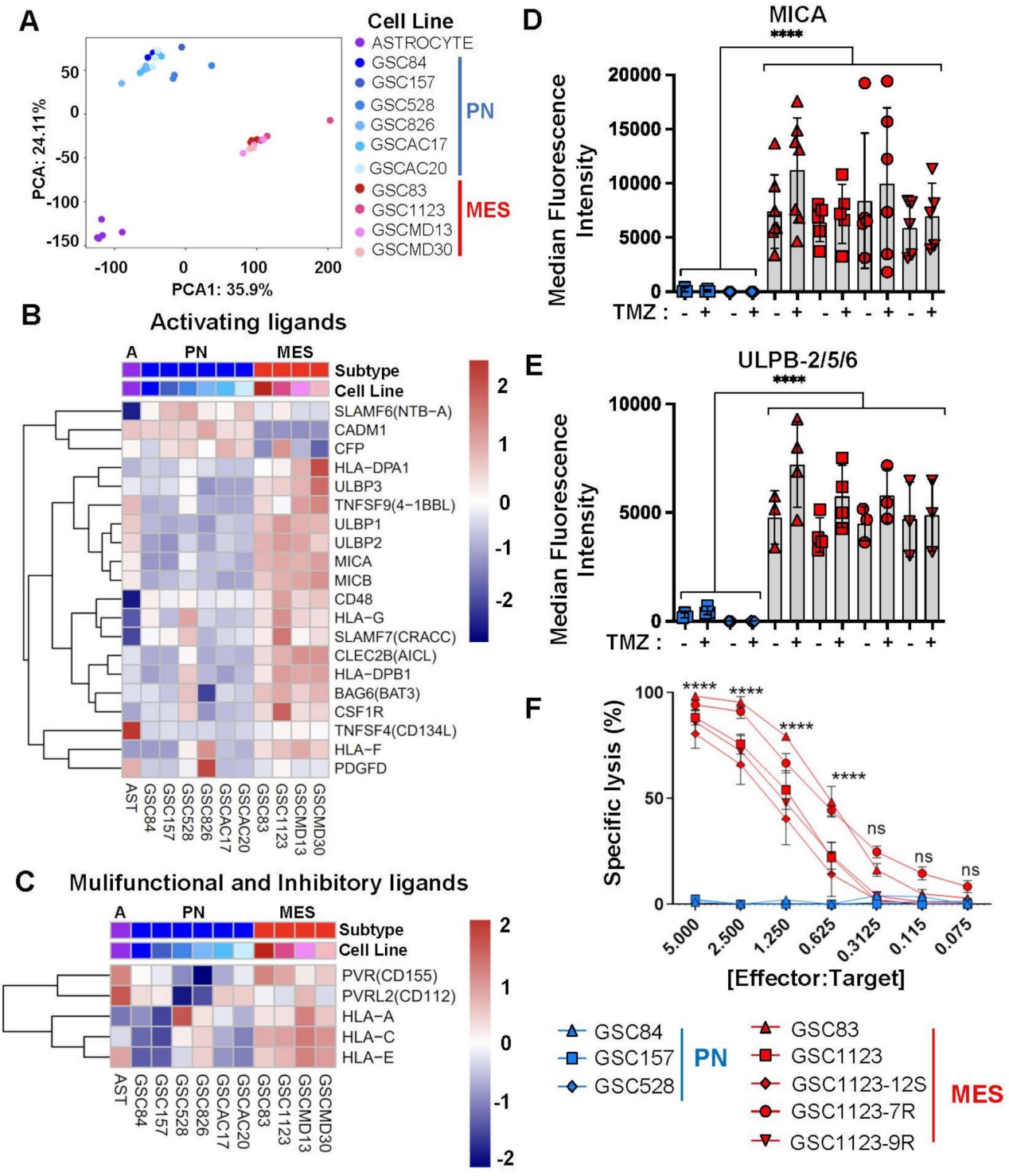

Fig. 1 Differential expression of NK cell ligands and susceptibility to NK cell-mediated cytotoxicity between patient-derived mesenchymal and proneural glioma stem cell populations. (**A**) Principal component analysis (PCA) of total transcriptomes of indicated cells: proneural GSCs (PN), mesenchymal GSCs (MES) and astrocytes. (**B-C**) In silico analysis of mRNA expression levels (microarrays) for NK cell ligands in a panel of PN and MES GSCs and Astrocytes. Activating NK ligand transcripts (**B**) and transcripts for multifunctional NK ligands (**C**). (**D-E**) Differential cell surface expression of NK ligands interacting with cytotoxic NKG2D by MES-GSCs and PN-GSCs (FACS); MICA (**D**) and ULBP-2/5/6 (**E**). GSCs were assayed with or without pretreatment with temozolomide (TMZ). MICA and ULBP-2/5/6 protein levels were expressed as median fluorescent intensity +/- SEM, for $n = 3–5$ independent repetitions, p values were determined for group comparisons by unpaired two-tailed t-test, $p < 0.0001$ (**F**) NK cell specific target cell (GSC) lysis analyzed by bioluminescence assay. GSCs were incubated with NK92MI human immortalized NK cells for 4 h at indicated ratios. Experiments were performed at least 3 times, **** $p < 0.0001$ as determined for group comparison between PN and MES time points by one way ANOVA with Tukey's multiple comparison test +/- SEM

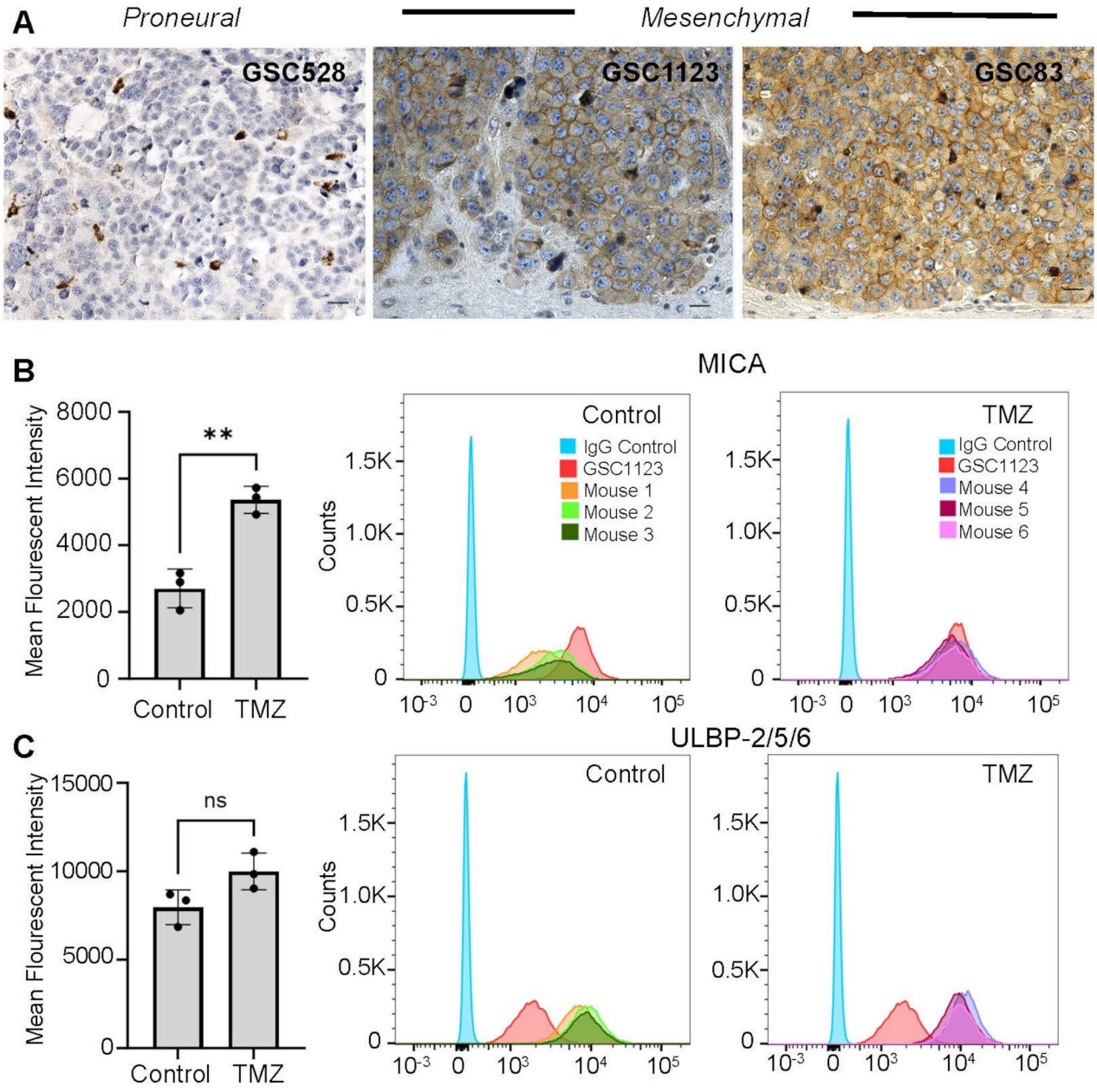

Fig. 2 NK cell ligand expression by intracranial GSC xenografts in the presence or absence of temozolomide therapy. (**A**) MICA immunohistochemical staining of proneural (GSC528) and mesenchymal (GSC1123 and GSC83) intracranial xenografts in SCID mice (magnification = 200X (size bar = 50 µm). (**B-C**) FACS analysis of NK ligand expression in dissociated GSC1123 intracranial tumours. MICA (**B**) and ULBP-2/5/6 (**C**) expression by cancer cells in mice either untreated (Control) or 48 h post temozolomide (TMZ) treatment. Mean fluorescence intensity +/- SEM (right side panels in **B** and **C**) and corresponding FACS histograms; Unstained GSC123 cells (blue), MICA- or ULBP-2/5/6-stained GSC1123 control cells from culture (red), and three independent stained GSC1123 cell populations ($n = 3$) isolated from untreated (light green, dark green and pink) or TMZ treated tumours (light purple, dark purple and dark blue). Statistical analysis by unpaired T-test, ** $p < 0.01$

(SCID) [5, 16, 47] or deficient (NSG) for NK cell activity (Fig. 3; fig. S10) [42, 55]. Both GSC subtypes efficiently triggered tumour formation in either strain of mice, with PN-GSCs exhibiting an expectedly slower growth kinetics and aggressiveness [20, 30]. We have earlier documented that in these settings, the exposure of tumour bearing NK-deficient NSG mice to TMZ produced a profound, but transient disease remission followed by a relapse of TMZ resistant and incurable lesions [20]. In order to examine the possible role of NK cells in this disease evolution process, NSG and SCID mice were inoculated with either MES-GSCs (GSC1123, GSC83) or PN-GSCs (GSC528) and upon tumour establishment the animals were exposed to a single dose of TMZ (120 mg/

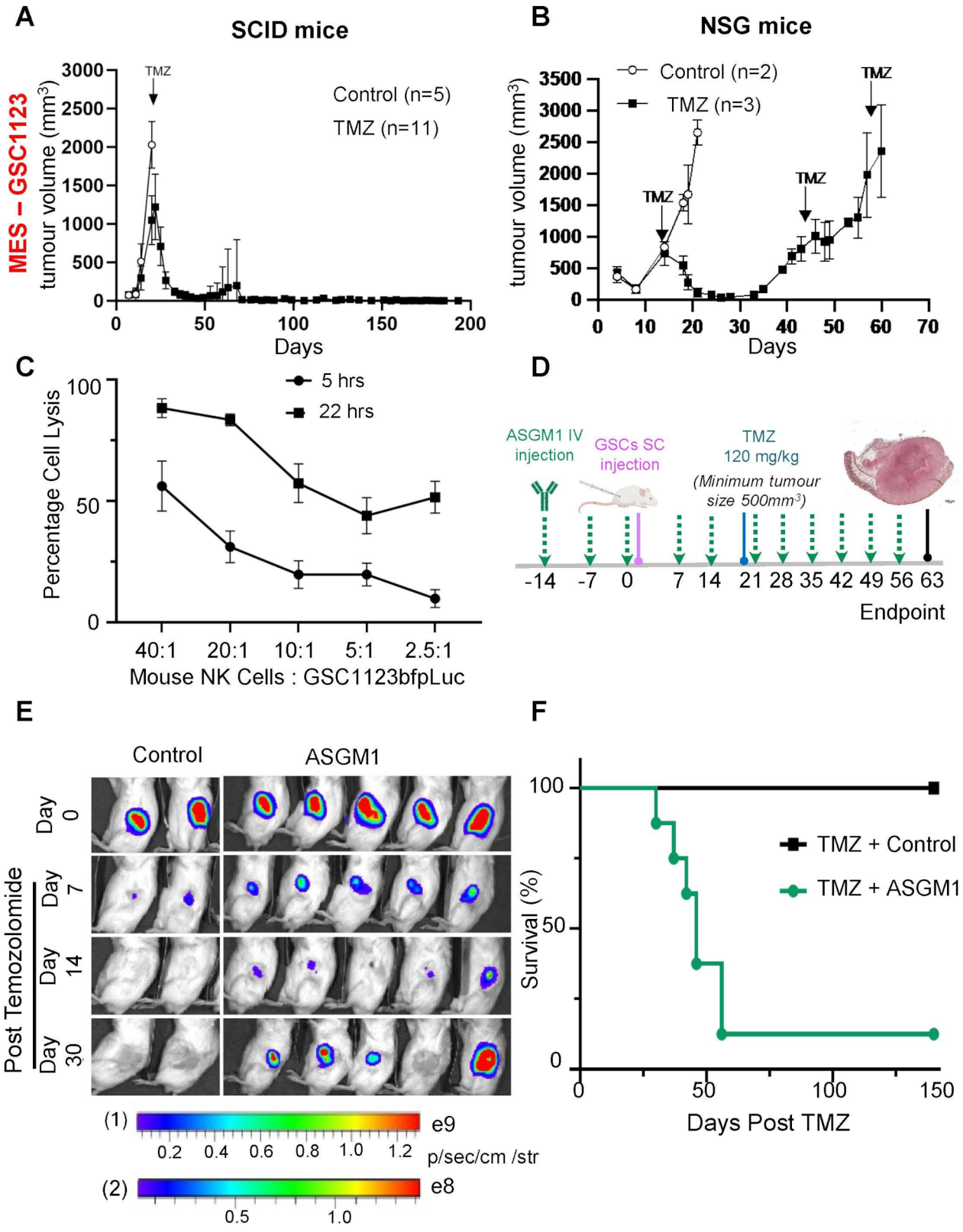

Fig. 3 (See legend on next page.)

(See figure on previous page.)

Fig. 3 Impact of endogenous mouse NK cells on post-chemotherapy recurrence of mesenchymal glioma stem cell xenografts. (**A**) Endogenous NK cell proficiency of SCID mice supports eradication of mesenchymal glioma stem cell (GSC1123) - driven subcutaneous xenografts by single dose of temozolomide (TMZ; 120 mg/kg); data expressed as mean +/- SD; (**B**) Endogenous NK cell deficiency of NSG mice is associated with post-TMZ relapse of GSC1123 subcutaneous xenografts (mean +/- SD); (**C**) Purified mouse NK cells efficiently kill GSC1123 mesenchymal glioma stem cells in vitro in a time dependent manner (BLI assay with readings conducted at 5 h and 22 h post NK treatment; mean value +/- SEM); (**D**) Experimental design to explore the effects of pharmacological NK inhibition (Asialo-GM1) on progression of mesenchymal GSC subcutaneous xenografts post TMZ-mediated tumour depopulation; (**E**) Asialo-GM1 treatment aborts TMZ-mediated GSC1123 tumour eradication in NK-proficient SCID mice– bioluminescent images; (**F**) Inhibition of endogenous NK cell cytotoxicity (Asialo-GM1) counteracts pro-survival effects of TMZ in NK-proficient SCID mice. Error is represented by SEM

kg i.p.). We observed that, as expected, in NK-deficient NSG mice this therapy resulted in a profound but transient tumour regression followed by a relapse of both MES-GSC and PN-GSC-driven lesions after approximately 40–50 days. This pattern was also recapitulated in NK-proficient SCID mice inoculated with PN-GSC cells (Fig. 3A-B; fig. S10B-E). However, in the case of SCID mice harbouring MES-GSC tumours the post-TMZ tumour relapse was completely aborted and the mice survived beyond 200 days without any evidence of active disease (Fig. 3A; fig. S10B). In contrast, PN-GSC-driven tumours continued to relapse in SCID mice (Fig. 3B; fig. S10D). To further ascertain that these effects can be attributed to the suggested capacity of mouse NK cells to recognize human cancer cell targets [7] and kill them [54] we isolated NKp46/NCR1-positive lymphocytes from mouse splenocyte preparations [53] (fig. S11) and performed bioluminescent cytotoxicity assays using human mesenchymal GSC1123bfpLuc glioma cells as targets. As expected, mouse NK cells were robustly cytotoxic against these GSCs (Fig. 3C). In several cases of surviving SCID mice a faint bioluminescent signal of residual MES-GSC cells was observed several months post TMZ therapy in the absence of progressive disease (fig. S12A-C), suggesting a possible contribution of tumour cell dormancy to anticancer effects of endogenous NK cells [15]. Collectively, these observations are consistent with the notion that MES-GSCs (but not PN-GSCs) are sensitive to NK cell effects in vivo. Moreover, since both NSG and SCID mice support the unperturbed tumour growth, TMZ-dependent tumour depopulation appears to be required for endogenous murine NK cells to exert an effective surveillance over the residual MES-GSCs, resulting in GSC subtype-specific obliteration of disease re-initiation.

Pharmacological targeting of NK cells overrides tumour eradication post chemotherapy

In order to further explore the role of innate immunity in curative effects of TMZ in NK-proficient SCID mice the animals bearing MES-GSC xenografts were depleted for NK cells using anti-AsialoGM1 (anti-NK) antibody [32] (Fig. 3D-F). Two weeks prior to cancer cell inoculation, SCID mice were randomized and subjected to weekly i.v. injections of either anti-Asialo-GM1, or vehicle for a total of 9 weeks. On day 14 of this cycle, all mice were subcutaneously inoculated with cancer cells (GSC1123) and once the tumours became established (500 mm^3) a single dose of TMZ (120 mg/kg) was injected i.p. followed by monitoring tumour responses (BLI, palpation) (Fig. 3D). In keeping with the aforementioned observations, TMZ exhibited a curative effect in control NK cell-proficient SCID mice, as indicated by disease free survival that extended beyond 150 days for the entire cohort. Notably, anti-Asialo-GM1 treatment reversed this effect almost completely with the majority (7/8) of mice exhibiting gradual tumour recurrence resulting in endpoint within less than 56 days post TMZ (Fig. 3E-F; fig. S13). These results further suggest that in SCID mice harbouring MES-GSC xenografts the endogenous NK activity is functionally required for tumour eradication and long-term survival post TMZ-dependent cancer cell depopulation. Thus, in mice depleted for NK cells either genetically (NSG strain) or pharmacologically (Asialo-GM1) the post-TMZ long-term survival is disrupted by tumour recurrence.

Recruitment of NK cells into the tumour mass in the course of temozolomide-induced regression

In order to visualise cellular events associated with TMZ-induced tumour regression, followed by either relapse, or cure in NSG or SCID mice, respectively, MES-GSC xenografts were subjected to serial histological examination (fig. S14A, B). As expected, a single dose of TMZ triggered a progressive loss of cellularity and dramatic shrinkage of the tumour mass in both NSG and SCID mice over a period of 2–3 weeks, after which cancer cell deposits became virtually undetectable until recurrence (in NSG mice only, fig. S14B). During this time tumour remnants in SCID mice exhibited a biphasic influx of mouse NCR1-positive NK cells peaking on days 3 and 14 post TMZ (fig. S15), with infiltrating NK cells forming thick rims around necrotic tumour regions and at the boundaries of regressing cancer cell deposits and surrounding stromal tissue. While scarce NCR1 staining was also detected in tumours harboured by NK-deficient NSG mice, no robust infiltration has occurred in this setting in agreement with the underlying NK cell maturation defect [1]. However, in both strains of mice the microenvironment of regressing tumours attracted other bone marrow derived, mouse, CD45-expressing cells (fig. S16). Microvascular density highlighted by CD31 staining was not visibly different between tumours in SCID and NSG

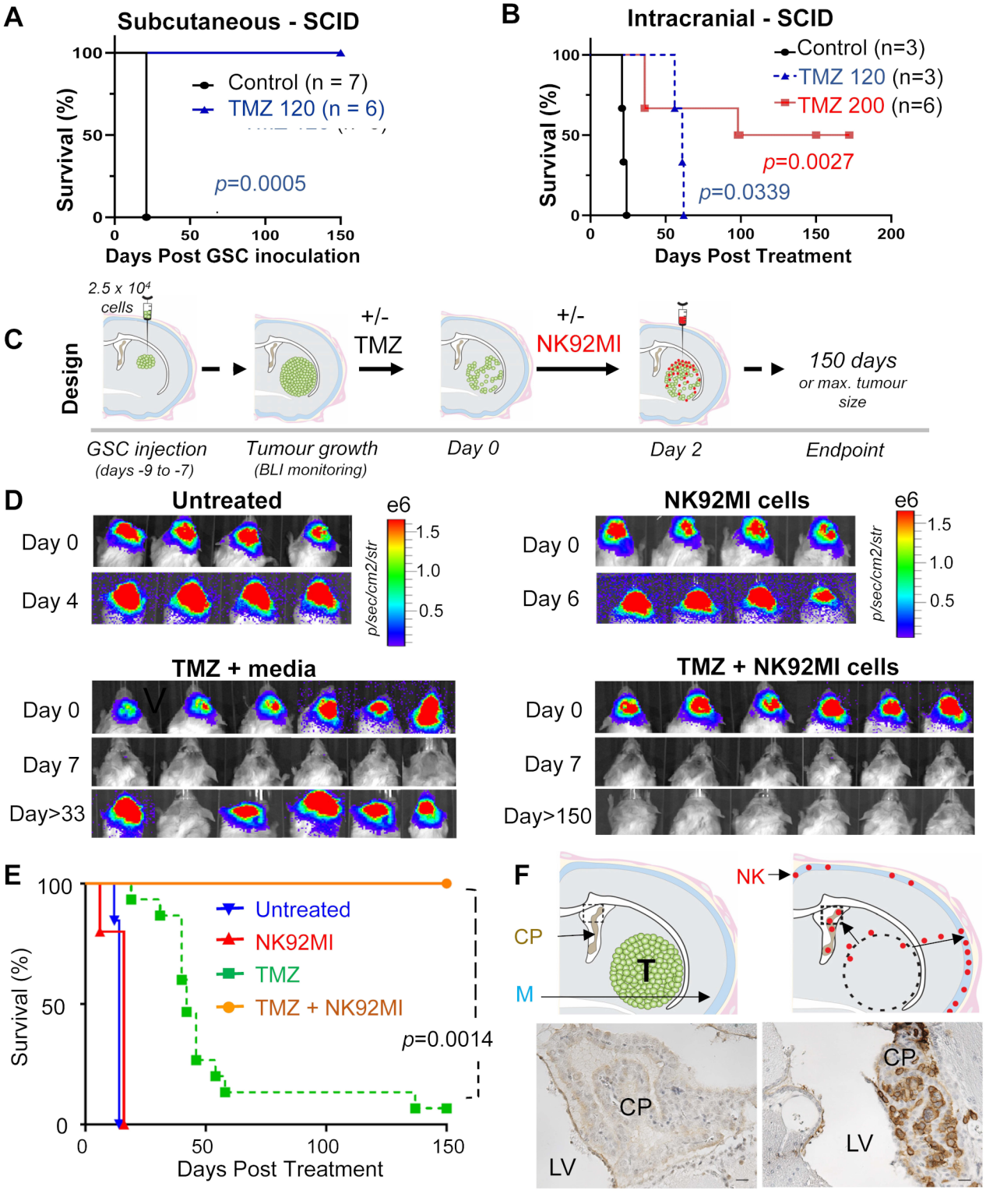

Fig. 4 (See legend on next page.)

(See figure on previous page.)

Fig. 4 Intracranial delivery of exogenous NK cells blocks post-temozolomide recurrence of mesenchymal glioma xenografts. (**A**) Kaplan-Meier curves indicating responsiveness of subcutaneous GSC1123 xenografts to TMZ treatment (120 mg/kg, i.p) in SCID mice. (**B**) Kaplan-Meier curves documenting relative refractoriness of intracranial GSC1123 xenografts to TMZ therapy (120 or 200 mg/kg i.p.) in SCID mice. (**C**) Experimental design of intracranial NK92MI therapy. (**D**) BLI representative scans of SCID mice in indicated treatment groups: untreated, NK92MI, TMZ + Media or TMZ + NK92MI. (**E**) Kaplan-Meier curves of GSC1123 tumour bearing mice for corresponding treatment groups show efficacy of TMZ and NK92MI combination. Statistical analysis was conducted by Curve comparison using the Gehan-Breslow-Wilcoxon test. Untreated group ($n = 13$ mice, 2 repeats), NK92MI treated group ($n = 5$ mice, 1 repeat), TMZ + media group ($n = 15$ mice, 4 repeats), TMZ + NK92MI group ($n = 6$ mice, 2 repeats). (**F**) Distribution of exogenous NK92MI cells in the brain of mice with GSC1123 xenografts: untreated (left) and TMZ + NK92MI treated mice (right) showing infiltration of NK92MI cells (brown) into the choroid plexus (CP) of lateral ventricle (LV) and meninges (M) 150 days post treatment

mice and even increased somewhat, as expected, with ongoing depopulation of viable cancer cells between capillaries (fig. S17). Overall, these observations suggest that in both NK cell-proficient and -deficient mice the MES-GSC xenografts underwent protracted and nearly complete regression post TMZ treatment. This process was paralleled by waves of NK cell infiltration, which were largely restricted to SCID mice.

Intracranial microenvironment restricts NK cell impact on post-chemotherapy survival of tumour bearing mice

The brain microenvironment uniquely restricts the access of drugs [37] and immune cells [49] to the tumour site resulting in their diminished anticancer activities. To explore this factor in the context of NK-sensitive MES-GSCs xenografts (Fig. 4A, B), these cells were inoculated intracranially [20] into NK cell-proficient SCID mice. Upon tumour establishment (as defined by the BLI signal) the mice received TMZ intraperitoneally at either a standard experimental dose of 120 mg/kg, or at increased dose of 200 mg/kg (Fig. 4B), established to compensate for reduced drug penetration into the brain [21, 35, 37]. Strikingly, neither of these TMZ treatment regimens recapitulated the dramatic prolongation in survival of tumour bearing SCID mice observed when the tumours were grown subcutaneously (Fig. 4A). Even at the higher dose of TMZ (200 mg/kg) only approximately 50% of mice survived longer than 150 days, while the remaining mice experienced tumour relapse before day 100 (Fig. 4B). These results are in agreement with reports suggesting a poor presence of NK cells in the brain tumour parenchyma [49], which is also consistent with our observations suggesting a limited representation of mouse CD45+, or NCR1 + cells in MES-GSC intracranial xenografts in SCID mice prior to treatment (fig. S18). Thus, the curative potential of NK cells during post-TMZ evolution of MES-GSC tumours is likely curtailed by poor access of these cells into the brain.

Intracranial NK cell therapy following temozolomide-mediated cytoreduction eradicates orthotopic mesenchymal glioma stem cell xenografts

Although the mechanism of endogenous NK cell exclusion from the brain tumour parenchyma remains poorly understood, one avenue to circumvent this barrier is through a direct intracranial immunotherapy [6, 24]. We set out to explore whether this approach could re-open the post-TMZ window of curative opportunity in the case of MES-GSC-driven tumours. MES-GSCs were inoculated intracranially into SCID mice and tumours were allowed to emerge (as BLI signal), at which point the mice were exposed to TMZ (120 mg/kg) followed two days later by injection of live human NK-like cell line, NK-92MI (Fig. 4C). These cells are engineered to remain in an activated state by constitutive expression of interleukin 2 (IL2) [46] and were approved by Food and Drug Administration (FDA) for experimental anticancer therapy in clinical trial settings [33]. Moreover, in our hands NK92MI cells exhibited a robust in vitro cytotoxicity against MES-GSC lines, but not against their PN-GSC counterparts (Fig. 1F). SCID mice were used as tumour recipients, as in these mice intracranial MES-GSC xenografts are not efficiently infiltrated by endogenous NK cells and are not eradicated following TMZ chemotherapy alone (Fig. 4B). Remarkably, the intracranial injection of NK92MI cells following TMZ chemotherapy radically changed the natural history of MES-GSC (GSC1123) tumours, resulting in tumour regression and long-term survival (> 150 days). This outcome is in contrast to the lethality of mice that received no therapy, or were injected only with NK92MI cells, or with TMZ alone, with "media" to serve as a surgical control (Fig. 4D, E; fig. S19). Histological examination of brains from all experimental groups showed infiltration of some mouse CD45 + cells and a scarce influx of endogenous NCR1 + mouse NK cells into the regressing tumour masses regardless of treatment (fig. S18). A global morphological overview documented end stage tumours in all groups except for the TMZ + NK92MI treated mice in which no tumours were detectable (fig. S19). Moreover, intracranial mesenchymal xenografts (GSC1123, GSC83) continued to express high levels of NK ligands, such as MICA and ULBP-2/5/6 in situ (Fig. 2; fig. S8A), in contrast to their proneural counterparts (GSC528), which remained negative for these molecules. This expression was somewhat increased by, but did not depend upon, the exposure to TMZ (fig. S8B, C). Overall, these results suggest that neither endogenous NK cells, nor exogenous NK92MI cells alone, even when injected intracranially, are able to prolong survival of MES-GSC brain tumour

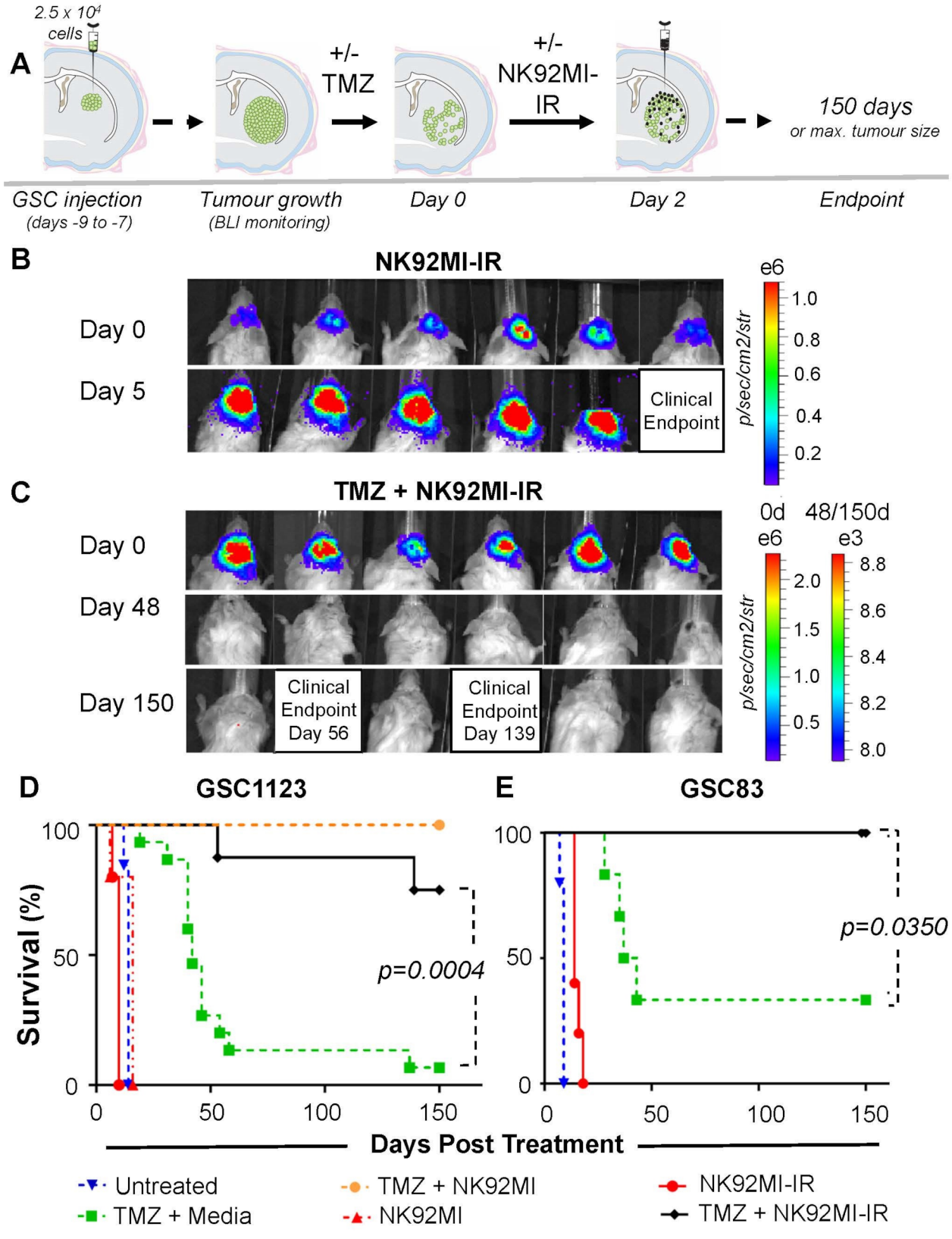

Fig. 5 (See legend on next page.)

(See figure on previous page.)

Fig. 5 Improved survival of brain tumour bearing SCID mice following combination therapy with temozolomide and irradiated NK92MI-IR cells. (**A**) Experimental protocol involving GSC1123-initiated brain tumours in SCID mice and therapy with systemic TMZ and intracranial injection of irradiated NK-92MI cells (NK92MI-IR). (**B-C**) Examples of BLI imagery of brain tumour formation and therapeutic response to indicated agents. (**D**) Kaplan-Meier survival curves of mice bearing GSC1123 tumours and treated with NK92MI-IR cells alone ($n=5$, 1 repeat) or combination therapy of TMZ + intracranial NK92MI-IR ($n=8$, 2 repeats). These results are overlayed with previously collected GSC1123 survival data, including: untreated mice ($n=13$), NK92MI alone ($n=5$), TMZ + media ($n=15$) and TMZ + NK92MI ($n=8$). (**E**) Kaplan-Meier survival curves for SCID mice with GSC83 intracranial xenografts including: untreated tumour bearing mice ($n=5$) and treatments with NK92MI-IR cells ($n=4$), TMZ + media ($n=6$, 3 repeats) or combination therapy of TMZ + NK92MI-IR ($n=5$, 2 repeats) cells. Statistical analysis comparing groups: TMZ + Media vs. TMZ + NK92MI-IR, for both, GSC tumour models, was conducted by curve analysis using the Gehan-Breslow-Wilcoxon test

bearing SCID mice, unless NK92MI therapy is combined with TMZ-mediated tumour depopulation.

Curative effects of lethally irradiated NK92MI cells combined with TMZ in mice harbouring mesenchymal glioma stem cell xenografts

Although NK92MI cells are FDA approved for human trials and exerted curative effects in MES-GSC-driven brain tumours, they are immortalised, transformed and thereby may pose inherent biosafety risks. Notably, NK92MI cells were detectable in brains of ostensibly cured (brain tumour-free) mice earlier inoculated with MES-GSCs (GSC1123; Fig. 4F and fig. S20). In some experiments these cells exhibited signs of neoplastic expansion throughout cerebral structures (fig. S21). One approach to decouple cytotoxicity of NK92MI cells from their proliferative potential relies on sublethal irradiation [28]. Exposure of NK92MI cells to radiation doses ranging from 2 Gy to 10 Gy was undertaken aiming to establish conditions that would maintain a sustained cell viability combined with cell cycle arrest (fig. S22A, B), which was achieved at 5 Gy. Indeed, following irradiation with 5 Gy NK92MI cells retained their structural integrity and viability for up to 7 days in vitro (fig. S22C), and they also remained selectively cytotoxic to MES-GSCs (fig. S22D). In order to test whether such irradiated NK92MI cells (NK92MI-IRs) are still able to prevent recurrence of TMZ treated MES-GSC xenografts, the respective cell lines (GSC1123, GSC83) were inoculated intracranially into SCID mice. Established tumours were then exposed to systemic TMZ (120 mg/kg), followed by intracranial NK92MI-IR therapy (Fig. 5A). Strikingly, this protocol resulted in aborted recurrence and long term survival of mice bearing GSC83 (5/5)(Fig. 5E and fig. S23 and S24B) or GSC1123 (4/6) (Fig. 5, B-D) xenografts, while neither TMZ alone (+media) nor NK92MI-IRs alone were able to achieve similar effects. There were no remarkable differences in the infiltration of the tumour mass with endogenous mouse CD45-positive bone marrow-derived cells, or NCR1-positive mouse NK cells, as a function of NK92MI cell injection (fig. S25A, B). GSC xenografts contained some mouse NCR1-positive cells in low abundance in all groups, with mice treated with TMZ alone being an intriguing, but presently unexplained exception (fig. S25C). Given the secretory activity of NK cells [36] we also assessed the impact of NK92MI-IR cell inoculation on the inflammatory and vascular components of the brain tumour microenvironment (fig. S26A-C). Apart from a modest and inconsistent increase in microvascular density (fig. S26A), no significant changes in microglia (Iba1) or leukocytic (CD45) content were observed following NK92MI inoculation (fig. S26B, C). Importantly, brain tissues recovered from mice that remained ostensibly tumour free following treatment with TMZ and NK92MI-IR revealed no remnants of cancer cells (fig. S27, fig. S28) or any obvious NK92MI-IR cell deposits. The latter was validated by staining of tumour tissues, or brain injection sites for anti-human CD45 antigen (fig. S29). These observations suggest that during their limited time of sustained viability in vivo, after irradiation and intracranial inoculation (post TMZ), NK92MI-IR cells were able to eliminate the residual MES-GSCs, avert disease recurrence and undergo their own spontaneous removal, an encouraging aspect of their biosafety.

TMZ and NK therapies cooperate within a limited time window

We observed that in mesenchymal GSC-driven brain xenografts the NK92MI-IR cell injection was only efficacious if preceded by depopulating TMZ therapy. This could result from chemotherapy reducing the ratio of viable residual GSC targets to NK92MI-IR effectors. If so, the opportunity to eliminate GSC by NK cells would be transient due to post-TMZ tumour repopulation, often accompanied by GSC drift toward TMZ resistance, as reported earlier [20]. To examine this possibility, intracranial GSC1123 xenografts were established in SCID mice, which then received TMZ therapy followed by intracranial delivery of NK92MI-IR cells either at a standard interval of 2 days, or at delayed time points, such as 7th, 14th, or 21st day post-TMZ (Fig. 6). Intriguingly, following the 2–7 day intervals between TMZ and NK92MI-IR injection, 9/12 mice were still alive and tumour-free at 150 days post treatment. In contrast, only 3/9 mice were tumour free in groups where NK92MI-IR injection was delayed until 14–21 days after TMZ treatment (Fig. 6B). To further ascertain that these effects could be attributed to the changing effector to target ratio the same numbers of mesenchymal GSB1123bfpLuc cells were mixed with NK92MI-IR effectors at different ratios and inoculated

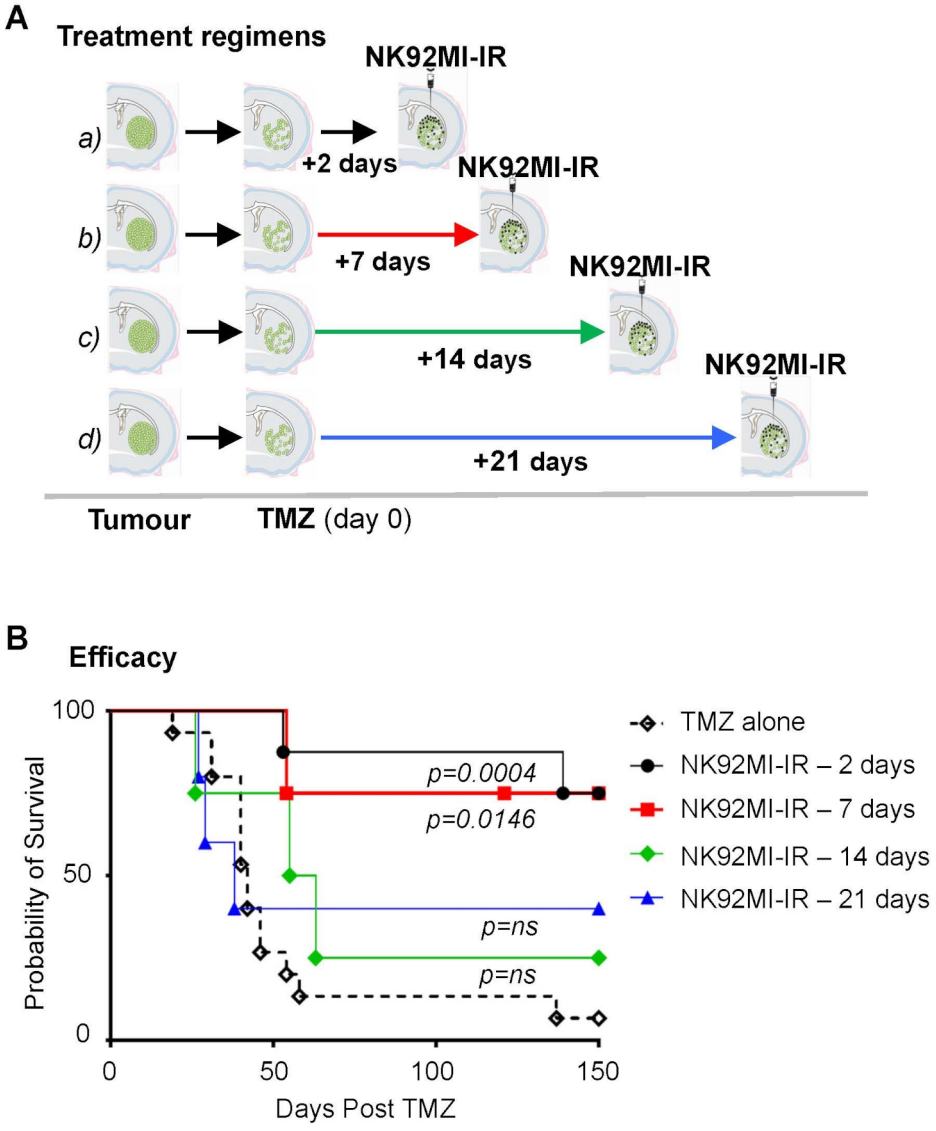

Fig. 6 Impact of NK cell therapy timing on their ability to prevent post-temozolomide relapse of intracranial mesenchymal glioma stem cell xenografts. (**A**) Experimental design to examine the effects of delay in NK92MI-IR intracranial injection relative to injection of TMZ to trigger tumour cell depopulation in GSC1123 brain xenografts; (**B**) Kaplan-Mejer symptom-free survival curves at different intervals between TMZ and NK92MI-IR therapies. Statistical analysis comparing groups: TMZ + media vs. TMZ + NK92MI-IR, for both, GSC tumour models, was conducted by curve analysis using the Gehan-Breslow-Wilcoxon test

intracranially into SCID mice without pre-exposure to TMZ (fig. S30). Remarkably, at 80:1 effector/target ratio NK92MI cells were able to abort the growth of cancer cells in vivo while at 10:1 ratio tumour onset was somewhat delayed, but still occurred in all mice as it did in untreated controls. This further suggests the ability of NK cells to control tumour growth in vivo only under certain numerical conditions. Collectively these results point to a window of curative opportunity, during which NK cells delivered directly into the tumour site after a successful cytoreductive chemotherapy may abort the disease relapse in a manner dependent on the molecular subtype and abundance of residual HGG-driving GSCs.

Discussion

Our present study suggests that in brain tumours driven by the mesenchymal subtype of human glioma initiating cells (MES-GSCs) a window of curative opportunity may exist following the initial response to TMZ chemotherapy and prior to overt tumour relapse. During this time interval the spontaneous influx, or therapeutic delivery of NK cells aborts the disease recurrence and results in unprecedented long-term (permanent) survival of xenograft

bearing mice. Notably PN-GSC xenografts were not responsive to the presence of NK cells and relapsed following initial TMZ depopulation. Indeed, subtypes of GSCs differed sharply in terms of their expression of NK ligands and so did bulk transcriptomes of HGGs (GBM) contained in the TCGA repository [51]. The implications of this pattern of response could be considerable, if biological and molecular determinants predisposing to meaningful NK cell effects could be identified and harnessed in the clinic.

More immediately, however, it is noteworthy that the effects of live NK92MI cells could be approximated through the use of their irradiated preparations, according to already established protocols [28, 33]. In this setting, following a single inoculation of irradiated NK92MI-IR cells they were completely eliminated from mouse brains within 7–10 days, and in combination with TMZ they still conferred a long-term survival upon MES-GSC xenograft bearing mice.

While in our study TMZ chemotherapy represents the backbone of experimental treatments, it is possible that the addition of NK cells may also cooperate with other cytoreductive modalities, such as alternative chemotherapy or radiation [51]. Exploring these possibilities represents an important, and presently unanswered challenge in view of the fact that approximately 50% of GBM patients exhibit up front resistance to TMZ [52]. TMZ resistance may also arise, as a consequence of the prolonged drug exposure [20, 48] and limit the applicability of the therapeutic paradigm suggested by the present study. Therefore, it is of great interest to understand the status and functionality of NK ligands in TMZ-resistant primary versus recurrent HGG and whether compatible cytoreductive options may exist in such settings. It is noteworthy that some of the isogenic sublines of GSC1123 cells tested in our study (GSC1123-7R, GSC1123-9R) have been previously selected for TMZ resistance in vivo [20] and they remain NK cell sensitive to the extent indistinguishable from controls (GSC1123-12 S) (Fig. 1F).

It should also be considered that individual human HGG tumours may contain both PN-GSCs and MES-GSCs, in various tumour subdomains [4], a circumstance that may require additional scrutiny in view of the apparent resistance of PN-GSCs to NK mediated killing. This noted, a global analysis of human GBM transcriptomes (TCGA) suggests that stratification of patients for greater NK ligand expression is feasible and tends to correlate with MES gene expression signature. The extension of this analysis to other subsets of HGG is, of course, of great interest.

Intriguingly, curative effects of the NK/TMZ protocol could be achieved in spite of the highly invasive properties of MES-GSCs and their ability to infiltrate the surrounding brain [2, 4]. It is presently unclear, whether exogenously delivered NK cells have the ability to migrate along similar paths as invading MES-GSCs and thereby eliminate them, or other mechanisms are involved in these effects. It is also of considerable interest that the effects of NK cells against susceptible GSCs could be enhanced by endogenous expression of cytokines such as IL-15 and especially IL-21, as recently demonstrated by Shanley et al. [40].

Finally, our results suggest that the efficacy of intracranial NK therapy post TMZ-dependent depopulation may be time-restricted. This is likely to be a function of the rapidity of tumour repopulation process from a state where residual cancer cells are beyond detection limits of bioluminescence to overt resurgence of macroscopic lesions, at which point event large numbers of NK cells become ineffective. This interpretation can be inferred from our experiments suggesting that NK cell-mediated prevention of GSC engraftment in vivo can only be achieved at effector to target ratio notably higher than that naturally existing in situ or those required for in vitro toxicity assays. Therefore, in our hands, curative effects of combined chemo-immunotherapy are only achieved if they are optimally timed.

While these possibilities are intriguing some of the limitations of our study merit future attention. They include the limited number of GSC lines available for our present study and the notion that given intrinsic heterogeneity of these cancer cells and their divergent properties [20], the exposure to non-curative NK therapy may elicit tumour evolution toward a NK resistant phenotype. While these are pressing experimental questions, our data suggest that NK therapy may have a place in treatment of at least a subset of GBM patients.

Conclusions

While several questions remain to be explored the profound effect of NK cells on post chemotherapy resolution of HGG lesions, within a defined time window, may signal an opportunity to harness the complementarities between innate immunity and cytoreductive treatment and change the dismal trajectory of this disease in a subset of patients.

Abbreviations

BBB	Blood–brain barrier
BLI	Bioluminescence
CNS	Central nervous system
GBM	Gioblastoma
GSC	Glioma stem cells
HGG	High grade glioma
i.c.	Intracranial, MES–GSC–mesenchymal glioma stem cells
NK cells	Natural killer cells
NSG	NOD/SCID/IL–2 g–/
PN	GSC–proneural glioma stem cells
s.c.	Subcutaneous
SCID	Severe combine immunodeficiency

TMZ Temozolomide

Supplementary Information

The online version contains supplementary material available at https://doi.org/10.1186/s40478-025-01984-3.

Supplementary Material 1

Acknowledgements
We are grateful for the advice and suggestions of our colleagues, especially, Dr. Patricia Areba, Dr. Dongsic Choi, Dr. Shankha Satpathy, Geoffroy Danieu and Laura Montermini. Finally, we are grateful to our families for their unwavering support.

Author contributions
Conceptualization: B. M., D. G., J. R.; Methodology: B. M., L. A., D. G., N. T., X. Z., S. H., I. N.; Investigation: B. M., L. A., D. G., X. Z.; Visualization: B. M., L. A., D. G.; Supervision: J. R., S. H., I. N.; Writing—original draft: B. M., J. R.; Writing—review & editing: B. M., L. A., D. G., N. T., S. H., I. N., J. R.

Funding
This work was supported through an operating grant from Canadian Institutes for Health Research (CIHR, PJT 183971), Canada Foundation of Innovation CAN Program (39799), Fondation Charles Bruneau (FCB) and Fondation CIBC– NET Program, Montreal Children's Hospital Foundation (MCHF)– NDR Program, Michael Whitehead and Louise Penny Endowment (MWLPE) and Jack Cole Chair in Pediatric Hematology/Oncology (all to JR). LA was supported by bursaries from MWLPE, Fonds de recherche du Quebec- Sante (FRQS) and RI MUHC Desjardins and McGil Faculty of Medicine stipend. FRQS provided institutional infrastructure support.

Data availability
No datasets were generated or analysed during the current study.

Declarations

Ethics approval and consent to participate
Not applicable.

Consent for publication
Not applicable.

Competing interests
The authors declare no competing interests.

Received: 24 August 2024 / Accepted: 10 March 2025
Published online: 21 March 2025

References

1. Abel AM, Yang C, Thakar MS, Malarkannan S (2018) Natural killer cells: development, maturation, and clinical utilization. Front Immunol 9:1869. https://doi.org/10.3389/fimmu.2018.01869
2. Adnani L, Kassouf J, Meehan B, Spinelli C, Tawil N, Nakano I, Rak J (2022) Angiocrine extracellular vesicles impose mesenchymal reprogramming upon proneural glioma stem cells. Nat Commun 13:5494. https://doi.org/10.1038/s41467-022-33235-7
3. Bagley SJ, Logun M, Fraietta JA, Wang X, Desai AS, Bagley LJ, Nabavizadeh A, Jarocha D, Martins R, Maloney E al (2024) Intrathecal bivalent CAR T cells targeting EGFR and IL13Rα2 in recurrent glioblastoma: phase 1 trial interim results. Nat Med 30:1320–1329. https://doi.org/10.1038/s41591-024-02893-z
4. Bastola S, Pavlyukov MS, Yamashita D, Ghosh S, Cho H, Kagaya N, Zhang Z, Minata M, Lee Y, Sadahiro H al (2020) Glioma-initiating cells at tumor edge gain signals from tumor core cells to promote their malignancy. Nat Commun 11:4660. https://doi.org/10.1038/s41467-020-18189-y
5. Bosma GC, Custer RP, Bosma MJ (1983) A severe combined immunodeficiency mutation in the mouse. Nature 301:527–530. https://doi.org/10.1038/301527a0
6. Burger MC, Zhang C, Harter PN, Romanski A, Strassheimer F, Senft C, Tonn T, Steinbach JP, Wels WS (2019) CAR-engineered NK cells for the treatment of glioblastoma: turning innate effectors into precision tools for cancer immunotherapy. Front Immunol 10:2683. https://doi.org/10.3389/fimmu.2019.02683
7. Champsaur M, Beilke JN, Ogasawara K, Koszinowski UH, Jonjic S, Lanier LL (2010) Intact NKG2D-independent function of NK cells chronically stimulated with the NKG2D ligand Rae-1. J Immunol 185:157–165. https://doi.org/10.4049/jimmunol.1000397
8. Chinot OL, Reardon DA (2014) The future of antiangiogenic treatment in glioblastoma. Curr Opin Neurol 27:675–682
9. Chiocca EA, Nassiri F, Wang J, Peruzzi P, Zadeh G (2019) Viral and other therapies for recurrent glioblastoma: is a 24-month durable response unusual? Neuro Oncol 21:14–25. https://doi.org/10.1093/neuonc/noy170
10. Chitadze G, Lettau M, Luecke S, Wang T, Janssen O, Fürst D, Mytilineos J, Wesch D, Oberg HH, Held-Feindt J et al (2016) NKG2D- and T-cell receptor-dependent lysis of malignant glioma cell lines by human γδ T cells: Modulation by temozolomide and A disintegrin and metalloproteases 10 and 17 inhibitors. Oncoimmunology 5:e1093276 https://doi.org/10.1080/2162402x.2015.1093276
11. Choe JH, Watchmaker PB, Simic MS, Gilbert RD, Li AW, Krasnow NA, Downey KM, Yu W, Carrera DA, Celli Aet al et al (2021) SynNotch-CAR T cells overcome challenges of specificity, heterogeneity, and persistence in treating glioblastoma. Sci Transl Med 13. https://doi.org/10.1126/scitranslmed.abe7378
12. Choi BD, Gerstner ER, Frigault MJ, Leick MB, Mount CW, Balaj L, Nikiforow S, Carter BS, Curry WT, Gallagher Ket al et al (2024) Intraventricular CARv3-TEAM-E T cells in recurrent glioblastoma. N Engl J Med 390:1290–1298. https://doi.org/10.1056/NEJMoa2314390
13. Chongsathidkiet P, Jackson C, Koyama S, Loebel F, Cui X, Farber SH, Woroniecka K, Elsamadicy AA, Dechant CA, Kemeny HR et al (2018) Sequestration of T cells in bone marrow in the setting of glioblastoma and other intracranial tumors. Nat Med 24:1459–1468 https://doi.org/10.1038/s41591-018-0135-2
14. Chuntova P, Chow F, Watchmaker PB, Galvez M, Heimberger AB, Newell EW, Diaz A, DePinho RA, Li MO, Wherry EJ al (2021) Unique challenges for glioblastoma immunotherapy-discussions across neuro-oncology and non-neuro-oncology experts in cancer immunology. Meeting report from the 2019 SNO immuno-oncology think tank. Neuro Oncol 23:356–375. https://doi.org/10.1093/neuonc/noaa277
15. Correia AL, Guimaraes JC, Auf der Maur P, De Silva D, Trefny MP, Okamoto R, Bruno S, Schmidt A, Mertz K, Volkmann Ket al et al (2021) Hepatic stellate cells suppress NK cell-sustained breast cancer dormancy. Nature 594:566–571. https://doi.org/10.1038/s41586-021-03614-z
16. Dorshkind K, Pollack SB, Bosma MJ, Phillips RA (1985) Natural killer (NK) cells are present in mice with severe combined immunodeficiency (scid). J Immunol 134:3798–3801
17. Dudley AC, Udagawa T, Melero-Martin JM, Shih SC, Curatolo A, Moses MA, Klagsbrun M (2010) Bone marrow is a reservoir for proangiogenic myelomonocytic cells but not endothelial cells in spontaneous tumors. Blood 116:3367–3371. https://doi.org/10.1182/blood-2010-02-271122
18. Frederico SC, Hancock JC, Brettschneider EES, Ratnam NM, Gilbert MR, Terabe M (2021) Making a cold tumor hot: the role of vaccines in the treatment of glioblastoma. Front Oncol 11:672508. https://doi.org/10.3389/fonc.2021.672508
19. Gangoso E, Southgate B, Bradley L, Rus S, Galvez-Cancino F, McGivern N, Güç E, Kapourani CA, Byron A, Ferguson KM al (2021) Glioblastomas acquire myeloid-affiliated transcriptional programs via epigenetic immunoediting to elicit immune evasion. Cell 184:2454–2470e2426. https://doi.org/10.1016/j.cell.2021.03.023
20. Garnier D, Meehan B, Kislinger T, Daniel P, Sinha A, Abdulkarim B, Nakano I, Rak J (2018) Divergent evolution of temozolomide resistance in glioblastoma stem cells is reflected in extracellular vesicles and coupled with radiosensitization. Neuro Oncol 20:236–248. https://doi.org/10.1093/neuonc/nox142
21. Hammond LA, Eckardt JR, Baker SD, Eckhardt SG, Dugan M, Forral K, Reidenberg P, Statkevich P, Weiss GR, Rinaldi DA et al (1999) Phase I and pharmacokinetic study of temozolomide on a daily-for-5-days schedule in patients with advanced solid malignancies. J Clin Oncol 17:2604–2613 https://doi.org/10.1200/jco.1999.17.8.2604

22. Hosseinalizadeh H, Habibi Roudkenar M, Mohammadi Roushandeh A, Kuwahara Y, Tomita K, Sato T (2022) Natural killer cell immunotherapy in glioblastoma. Discov Oncol 13:113. https://doi.org/10.1007/s12672-022-00567-1
23. Huntington ND, Cursons J, Rautela J (2020) The cancer-natural killer cell immunity cycle. Nat Rev Cancer 20:437–454. https://doi.org/10.1038/s41568-020-0272-z
24. Ishikawa E, Tsuboi K, Saijo K, Harada H, Takano S, Nose T, Ohno T (2004) Autologous natural killer cell therapy for human recurrent malignant glioma. Anticancer Res 24:1861–1871
25. Karimi MA, Lee E, Bachmann MH, Salicioni AM, Behrens EM, Kambayashi T, Baldwin CL (2014) Measuring cytotoxicity by bioluminescence imaging outperforms the standard chromium-51 release assay. PLoS ONE 9:e89357. https://doi.org/10.1371/journal.pone.0089357
26. Keskin DB, Anandappa AJ, Sun J, Tirosh I, Mathewson ND, Li S, Oliveira G, Giobbie-Hurder A, Felt K, Gjini Eet al et al (2019) Neoantigen vaccine generates intratumoral T cell responses in phase Ib glioblastoma trial. Nature 565:234–239. https://doi.org/10.1038/s41586-018-0792-9
27. Lim M, Xia Y, Bettegowda C, Weller M (2018) Current state of immunotherapy for glioblastoma. Nat Rev Clin Oncol 15:422–442. https://doi.org/10.1038/s41571-018-0003-5
28. Liu Q, Xu Y, Mou J, Tang K, Fu X, Li Y, Xing Y, Rao Q, Xing H, Tian Zet al et al (2020) Irradiated chimeric antigen receptor engineered NK-92MI cells show effective cytotoxicity against CD19(+) malignancy in a mouse model. Cytotherapy 22:552–562. https://doi.org/10.1016/j.jcyt.2020.06.003
29. Lupo KB, Matosevic S (2020) CD155 immunoregulation as a target for natural killer cell immunotherapy in glioblastoma. J Hematol Oncol 13:76. https://doi.org/10.1186/s13045-020-00913-2
30. Mao P, Joshi K, Li J, Kim SH, Li P, Santana-Santos L, Luthra S, Chandran UR, Benos PV, Smith Let al et al (2013) Mesenchymal glioma stem cells are maintained by activated glycolytic metabolism involving aldehyde dehydrogenase 1A3. Proc Natl Acad Sci U S A 110:8644–8649
31. Maskalenko NA, Zhigarev D, Campbell KS (2022) Harnessing natural killer cells for cancer immunotherapy: dispatching the first responders. Nat Rev Drug Discov 21:559–577. https://doi.org/10.1038/s41573-022-00413-7
32. Monnier J, Zabel BA (2014) Anti-asialo GM1 NK cell depleting antibody does not alter the development of bleomycin induced pulmonary fibrosis. PLoS ONE 9:e99350. https://doi.org/10.1371/journal.pone.0099350
33. Navarrete-Galvan L, Guglielmo M, Cruz Amaya J, Smith-Gagen J, Lombardi VC, Merica R, Hudig D (2022) Optimizing NK-92 serial killers: gamma irradiation, CD95/Fas-ligation, and NK or LAK attack limit cytotoxic efficacy. J Transl Med 20:151. https://doi.org/10.1186/s12967-022-03350-6
34. Neftel C, Laffy J, Filbin MG, Hara T, Shore ME, Rahme GJ, Richman AR, Silverbush D, Shaw ML, Hebert CMet al et al (2019) An integrative model of cellular states, plasticity, and genetics for glioblastoma. Cell 178:835–849e821. https://doi.org/10.1016/j.cell.2019.06.024
35. Ostermann S, Csajka C, Buclin T, Leyvraz S, Lejeune F, Decosterd LA, Stupp R (2004) Plasma and cerebrospinal fluid population pharmacokinetics of temozolomide in malignant glioma patients. Clin Cancer Res 10:3728–3736. https://doi.org/10.1158/1078-0432.Ccr-03-0807
36. Paul S, Lal G (2017) The molecular mechanism of natural killer cells function and its importance in cancer immunotherapy. Front Immunol 8:1124. https://doi.org/10.3389/fimmu.2017.01124
37. Pitz MW, Desai A, Grossman SA, Blakeley JO (2011) Tissue concentration of systemically administered antineoplastic agents in human brain tumors. J Neurooncol 104:629–638. https://doi.org/10.1007/s11060-011-0564-y
38. Reifenberger G, Wirsching HG, Knobbe-Thomsen CB, Weller M (2017) Advances in the molecular genetics of gliomas - implications for classification and therapy. Nat Rev Clin Oncol 14:434–452. https://doi.org/10.1038/nrclinonc.2016.204
39. Sabbagh A, Beccaria K, Ling X, Marisetty A, Ott M, Caruso H, Barton E, Kong LY, Fang D, Latha Ket al et al (2021) Opening of the blood-brain barrier using low-intensity pulsed ultrasound enhances responses to immunotherapy in preclinical glioma models. Clin Cancer Res 27:4325–4337. https://doi.org/10.1158/1078-0432.Ccr-20-3760
40. Shanley M, Daher M, Dou J, Li S, Basar R, Rafei H, Dede M, Gumin J, Pantaleón García J, Nunez Cortes AKet al et al (2024) Interleukin-21 engineering enhances NK cell activity against glioblastoma via CEBPD. Cancer Cell 42:1450–1466e1411. https://doi.org/10.1016/j.ccell.2024.07.007
41. Shimasaki N, Jain A, Campana D (2020) NK cells for cancer immunotherapy. Nat Rev Drug Discov 19:200–218. https://doi.org/10.1038/s41573-019-0052-1
42. Shultz LD, Lyons BL, Burzenski LM, Gott B, Chen X, Chaleff S, Kotb M, Gillies SD, King M, Mangada Jet al et al (2005) Human lymphoid and myeloid cell development in NOD/LtSz-scid IL2R gamma null mice engrafted with mobilized human hemopoietic stem cells. J Immunol 174:6477–6489. https://doi.org/10.4049/jimmunol.174.10.6477
43. Singh SK, Hawkins C, Clarke ID, Squire JA, Bayani J, Hide T, Henkelman RM, Cusimano MD, Dirks PB (2004) Identification of human brain tumour initiating cells. Nature 432:396–401
44. Singh K, Hotchkiss KM, Patel KK, Wilkinson DS, Mohan AA, Cook SL, Sampson JH (2021) Enhancing T cell chemotaxis and infiltration in glioblastoma. Cancers (Basel) 13. https://doi.org/10.3390/cancers13215367
45. Song E, Mao T, Dong H, Boisserand LSB, Antila S, Bosenberg M, Alitalo K, Thomas JL, Iwasaki A (2020) VEGF-C-driven lymphatic drainage enables immunosurveillance of brain tumours. Nature 577:689–694. https://doi.org/10.1038/s41586-019-1912-x
46. Tam YK, Maki G, Miyagawa B, Hennemann B, Tonn T, Klingemann HG (1999) Characterization of genetically altered, interleukin 2-independent natural killer cell lines suitable for adoptive cellular immunotherapy. Hum Gene Ther 10:1359–1373. https://doi.org/10.1089/10430349950018030
47. Viloria-Petit A, Miquerol L, Yu JL, Gertsenstein M, Sheehan C, May L, Henkin J, Lobe C, Nagy A, Kerbel RS al (2003) Contrasting effects of VEGF gene disruption in embryonic stem cell-derived versus oncogene-induced tumors. EMBO J 22:4091–4102
48. Wang J, Cazzato E, Ladewig E, Frattini V, Rosenbloom DI, Zairis S, Abate F, Liu Z, Elliott O, Shin YJ et al (2016) Clonal evolution of glioblastoma under therapy. Nat Genet 48:768–776 https://doi.org/10.1038/ng.3590
49. Wang Q, Hu B, Hu X, Kim H, Squatrito M, Scarpace L, deCarvalho AC, Lyu S, Li P, Li Y al (2017) Tumor evolution of glioma-intrinsic gene expression subtypes associates with immunological changes in the microenvironment. Cancer Cell 32:42–56e46. https://doi.org/10.1016/j.ccell.2017.06.003
50. Weiss T, Schneider H, Silginer M, Steinle A, Pruschy M, Polić B, Weller M, Roth P (2018) NKG2D-dependent antitumor effects of chemotherapy and radiotherapy against glioblastoma. Clin Cancer Res 24:882–895. https://doi.org/10.1158/1078-0432.Ccr-17-1766
51. Wen PY, Weller M, Lee EQ, Alexander BM, Barnholtz-Sloan JS, Barthel FP, Batchelor TT, Bindra RS, Chang SM, Chiocca EA al (2020) Glioblastoma in adults: a society for neuro-oncology (SNO) and European Society of Neuro-Oncology (EANO) consensus review on current management and future directions. Neuro Oncol 22:1073–1113. https://doi.org/10.1093/neuonc/noaa106
52. Wick W, Platten M (2014) Understanding and targeting alkylator resistance in glioblastoma. Cancer Discov 4:1120–1122. https://doi.org/10.1158/2159-8290.Cd-14-0918
53. Wong P, Wagner JA, Berrien-Elliott MM, Schappe T, Fehniger TA (2021) Flow cytometry-based ex vivo murine NK cell cytotoxicity assay. STAR Protoc 2:100262. https://doi.org/10.1016/j.xpro.2020.100262
54. Xie X, Brünner N, Jensen G, Albrectsen J, Gotthardsen B, Rygaard J (1992) Comparative studies between nude and scid mice on the growth and metastatic behavior of xenografted human tumors. Clin Exp Metastasis 10:201–210. https://doi.org/10.1007/bf00132752
55. Zamora AE, Grossenbacher SK, Aguilar EG, Murphy WJ (2015) Models to Study NK Cell Biology and Possible Clinical Application. Curr Protoc Immunol 110:14.37.11–14.37.14 https://doi.org/10.1002/0471142735.im1437s110

Publisher's note